

AKADÉMIAI KIADÓ

Visualization of the effect of TR100 anti-cancer compound on membrane nanotubes with SR-SIM microscopy

Resolution and
Discovery

6 (2021) 1, 12-19

DOI:

10.1556/2051.2022.00091

© 2022 The Author(s)

ALEXANDRA JÚLIA HENCZ¹, PÁL SOMOGYI²,
HENRIETT HALÁSZ³ and EDINA SZABÓ-MELEG^{3,4*} 

¹ Institute of Physiology, Medical School, University of Pécs, Pécs, Hungary

² Soft Flow Ltd, Pécs, Hungary

³ Department of Biophysics, Medical School, University of Pécs, Pécs, Hungary

⁴ Nano-Bio-Imaging Core Facility, Szentágotthai Research Centre, University of Pécs, Pécs, Hungary

Received: December 1, 2021 • Accepted: March 17, 2022

Published online: April 8, 2022

ORIGINAL RESEARCH
PAPER



ABSTRACT

One of the most dangerous diseases is cancer, nearly 2 million new cancer types are diagnosed each year, worldwide, causing most of the death. Therefore, cancer is in the focus of many types of research. To prevent the proliferation and spreading of malignant cells, several compounds have been developed in chemotherapy, however, a significant proportion of these have serious side effects, and resistance is commonly emerging early after administration. Tumor cells require tropomyosin-containing actin network for their growth and survival. The tropomyosin profile is considerably changed in cancers resulting in the dramatic rearrangements of the actin cytoskeleton structure, therefore anti-tropomyosin compounds can be a new perspective in cancer therapy, such as TR100 which was reported to be capable of destroying cancer cells in a highly tumor-specific manner by increasing the depolymerization of the actin filament. On the other hand tumor cells can commonly communicate with each other via membrane nanotubes (NTs) for which actin is essential for growth. Tumor cell NTs may transport not only signal molecules, or cell organelles, but resistance factors against chemotherapeutic agents to help to survive. Immune cells also frequently use membrane nanotubes for communication, therefore, in this study we focused on the visualization of the effect of TR100 on the morphology and formation of B lymphoma cell NTs with superresolution structured illumination microscopy. TR100 treatment caused spectacular changes on the NT forming capability and the morphology of B cells in a concentration dependent manner, while low concentration of the agent significantly promoted NT formation, and at the same time produced shorter and thicker tubes in the early stage of their formation, in higher concentration it affected mainly only the cells, causing the rounding and finally the death of them. We were not able to detect any significant change on cells with extended nanotubular network, suggesting that TR100 is a less potent candidate in anti-cancer therapy.

KEYWORDS

superresolution, microscopy, membrane nanotube, actin, B cell

1. INTRODUCTION

Cytoskeleton contributes to tumorigenesis since its proteins control the cell division, and may activate signal transduction and oncogenes. The actin is potentially the most vulnerable cytoskeletal element in tumor cells. Actin is a multifunctional protein, which can be found in all eukaryotic cells. It has role in a wide variety of cellular processes, e.g. it is involved in the contraction of muscles, in the migration of cells, in the maintenance of the shape of the cells, in mitosis, in different transport processes (e.g. cell organelles, vesicles), or in the formation of cell protrusions (e.g. lamellipodia, filopodia). These functions are regulated by actin-binding proteins (e.g. myosin, formin, cofilin, tropomyosin).

Based on invited lecture presented at the HSM 2021 Conference.

*Corresponding author.

E-mail: edina.meleg@aok.pte.hu



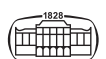
Connection and communication between cells and organs are important in the creation and maintenance of a supercellular organization. Direct cell-cell communication is crucial for eukaryotic cells [1] to survive and to occupy their normal function. This cross talk takes place frequently by membrane protrusions (e.g. filopodia) appearing on the surface of the cells. These projections are exceptionally heterogeneous structures facilitating not only communication and matter transport, but cell migration, exocytosis, sensing, wound healing, cell-cell interaction, as well as viral and bacterial infection. A group of these protrusions, the membrane nanotubes (NTs) provide physical connection even between distant cells. These transient structures support cell-to-cell communication and intercellular exchange of information [2] by the transfer of cell organelles (lysosomes, mitochondria), lipids, proteins, vesicles, DNA/RNA molecules, pathogens as viruses and bacteria. Despite the fact that more and more is known about membrane nanotubes, the molecular mechanism of their formation is not completely understood as different models are existing for NT growth. Formation of NTs can be described with two possible mechanisms [3]. The first model describes the NTs as actin-driven membrane protrusions, where from a filopodium-like projection a thin bridge is formed due to actin polymerization to couple with other cells [4]. In NTs actin is organized into bundles of polarized filaments and can create extensive network due to polymerization. Although actin polymerization is crucial in the initiation of NT growth, some actin-binding regulators are also in focus during NT formation, such as I-BAR as an inducer and stabilizer of membrane projections, proteins of the Rho GTPase family (e.g. CDC42, Rac1) as facilitators of actin rearrangement, VASP as a trigger of actin nucleation and Eps8 as stabilizer of actin bundles in the growing protrusion. According to the second proposed mechanism of NT development, cells separate from each other after close contact (e.g. in cell division cell dislodgement is followed by the retention of a thin membrane extension) retain a membrane tether that develops to an actin-based NT [5]. Considering that NTs are associated with disease conditions, the description of signals involved in the maintenance and particularly in the formation of NTs is crucial. It was proved that stress (e.g. hydrogen peroxide treatment) affects NT formation [6] by the activation of the p53, the Akt/PI3K/mTOR and the MAPK [7] signaling pathways. However, the results of these stress experiments are controversial, because stress conditions increasing NT formation do not affect all cells the same way (e.g. in astrocytes and neurons stress effects increase NT formation originated from the stressed cells, while in endothelial cells stress leads to an increased formation of NTs from the non-stressed cells) [8]. Literature suggests involvement of different signaling pathways in NT growth initiation, but only the M-sec- and LST1-linked [9] pathways were found to have somewhat general importance in this process, independent of cell type. Actin dependent myosin 10 was also suggested as a factor controlling NT formation, as overexpression of myosin 10 in neuronal cells leads to increased NT number [6, 10]. NTs are frequently

addressed as elongated filopodial structures, interestingly, but key regulatory complexes of filopodia formation (CDC42/IRSp53/VASP or Eps8) acting as positive initiators of filopodial growth have negative effect on inception of NTs and decrease their number between cells [11, 12]. Furthermore, inflammatory cytokines (e.g. TNF-alpha) were described to be able to inhibit NT formation between cancer cells [13]. Thus, many candidates associated with nanotube formation were identified, due to the fact that the mechanisms of NT-growth are highly diverse even within an identical way of NT formation.

Although, membrane nanotubes are transient structures, their lifetime is diverse, they can exist from several minutes to a couple of days [4]. Among others, the cells of the immune system also frequently use membrane nanotubes to transfer different signals thus may mediate different immune functions. It is known that key components of the humoral immune response, the mature B cells spontaneously form extensive nanotubular network but only under physiological circumstances (37 °C, 5% CO₂) [14]. It is also hypothesized that B cells may activate the T cell dependent immune response via NTs [14, 15]. Actin is the main cytoskeletal component of B cells NTs and has essential role in the formation of them, treatment of B cells with actin-depolymerizing drugs (e.g. latrunculin) even at relatively low concentrations (0.5–1 μM) inhibits and at higher concentrations (2–5 μM) almost completely blocks NT growth [14].

Tumor cells were also observed to communicate via NTs. It is supposed that NTs play role in the migration and metastasis of malignant cells. Oncogenic miRNA-transfer was detected via direct nanotubular connections between tumor and normal (healthy) cells, and as a response to radiotherapy microparticles produced by cancer cells passed through NTs [16]. Transfer of resistance factors against chemotherapeutic agents via NTs was also published [17].

Tumor cells rely on the cytoskeletal elements (e.g. intermediate filaments, microfilaments/actin/) and their associated proteins (e.g. tropomyosins) for their growth and survival. Actin monomers are held by weak bonds which enable the rapid assembly (actin monomer incorporation) and disassembly (actin monomer release) of actin network thus facilitate cells to migrate. Tropomyosin (Tpm) is an integral part of the actin filament and can be found mostly in all cell cytoskeleton. In striated muscles Tpm's mediate the access of myosin 2 to the actin filament thus aid muscle contraction, in non-muscle cells they have pivotal role in the actin filament stabilization (make the filament stronger and less fragile), but also control the association of actin-binding proteins to actin. Tropomyosins are dimers of coiled-coil proteins that bind along the side of the actin filament, spanning six-seven actin subunits. It was published that the expression level of some tropomyosins show significant change in tumor cells, high-molecular-weight (HMW) ones suffer significant decrease [18–21], leading to the decrease both in the mRNA levels and in the synthesis of HMW isoforms (as Tpm 2.1, Tpm 1.4, Tpm 1.6 and Tpm 1.7), while the expression levels of some low-molecular-weight (LHW) tropomyosins, especially Tpm 3.1 and Tpm 4.2. isoforms



(key players of cell motility in metastasis) are elevated [22–24], suggesting that tropomyosins have fundamental role in the actin remodeling during malignant transformation, and facilitate tumor cell metastasis [25, 26] thus affect tumor cell survival growth. This is supported by the fact that e.g. Tpm 3.1 isoform has role in the maintenance of cortical actin integrity in cell division, and it also stabilizes the actin cytoskeleton [27] consequently influences cell motility and contraction. As a result, anti-tropomyosin drugs are potential and promising anti-cancer candidates by disrupting the cytoskeleton of cancer cells.

TR100 is a recently developed anti-tropomyosin compound targeting the Tpm isoforms which regulate a wide range of physiological processes, as e.g. actin-myosin interaction [28], calcium-uptake or calcium-blocking [29]. TR100 changes actin dynamics, as it raises the Tpm 3.1. depolymerization role on actin but leaves unchanged the actin-tropomyosin binding. It was reported that in experiments conducted to devastate tumor cells, TR100 effectively disrupted not only the target's cytoskeleton but also destroyed the whole cell. Studies conducted on neuroblastoma, melanoma and cardiac cell line suggested that TR100 has no effect on healthy cells and only malignant cells are destroyed by causing the regression of growth of cancer cells. On the other hand, TR 100 did not inhibit or affect normal cardiac cell contractility [30, 31] demonstrating that TR100 is highly selective and has the ability to reduce only the target tumor cell growth without influencing any normal cell function. Furthermore, higher TR100 concentration (50 μM) changed the length, the elongation, as well as the depolymerization of actin filaments [31]. In contrast, several other anti-cancer drugs were used against neuroblastoma, e.g. vinca alkaloids such as vincristine, but while those alkaloids disrupt the tubulin monomers both in malignant and healthy cells, TR100 was able to selectively destroy only cancer cells [32]. The great advantage of TR100 over the other anti-cancer agents is its selectivity, as it shows preference to tropomyosin, more specifically its Tpm 3.1 isoform.

It was proved that tumor cells can communicate with each other via actin-containing membrane nanotubes to help to survive. Isolated tumors can be destroyed due to chemo- or radiotherapy, although it was published that tumor cells connected to each other with membrane nanotubes survived the anti-cancer treatment, even the number of intercellular NTs was increased after the therapy [33]. As TR100 is a potential chemotherapeutic agent and immune cells frequently use membrane nanotubes for communication, we focused on the visualization of the effect of TR100 cancer cell antagonist principally on the morphology and formation of NTs developed among murine B lymphoma cells. Our results are contradictory, TR100 showed effects only in the early phase of NT growth, however no remarkable changes were observed on cells with advanced nanotube networks even at high concentration of TR100. According to our knowledge, this is the first publication to provide data on the effect of TR100 on membrane nanotubes and on B cells.

2. EXPERIMENTAL DETAILS

Experiments were done principally to reveal the number of NTs, and the changes of the actin pattern in B cells due to TR100 treatment. Different concentrations of TR100 were used on murine B cells of reticulum cell sarcoma to reveal its effect on the nanotubes' morphology and their actin network. Alterations were visualized by Zeiss Elyra S1 superresolution structured illumination microscopy (SR-SIM, $d_{\text{lat}} \sim 80\text{--}90\text{ nm}$).

Control and TR100 treated samples were prepared on the same day parallelly. A20 mature B cells of mouse malignant tumor (ATCC TIB208, I-Ad/Ed+) were cultured in RPMI-1640 medium, supplemented with 2 mM L-glutamine (Lonza, Basel, Switzerland), 1 mM Na-pyruvate (Lonza, Basel, Switzerland), 50 μM 2-mercaptoethanol (Sigma-Aldrich, St. Louis, MO, USA), antibiotics and 10% FBS (Sigma-Aldrich, St. Louis, MO, USA), and were kept at 37 °C in 5% CO₂ incubator. To study B cell nanotubes borosilicate bottomed chambers (P35G-0.170-14-C MatTek In Vitro Life Science Laboratories, Bratislava, Slovak Republic) were coated with 10 $\mu\text{g mL}^{-1}$ fibronectin (Sigma-Aldrich, St. Louis, MO, USA), as optimal extracellular matrix support [14] overnight to model physiological circumstances. TR100 (kind gift from prof. Peter Gunning, UNSW, School of Medical Sciences, Sidney, Australia) was used two different ways in cell cultures: TR100 was added to the cells before or after the nanotube formation, cells were incubated for 2 h with different TR100 concentrations (2 and 20 μM), then fixed. The same amount of DMSO (Sigma-Aldrich, St. Louis, MO, USA) was used in the control experiments (to provide the same conditions, as TR100 is dissolved in DMSO). 10⁶ cells/well were incubated at these conditions. For each measurement 3 controls and 6 treated samples were used. Actin was labeled as described before [14], briefly: cells were fixed with 4% paraformaldehyde for 10 min, at room temperature (RT), then permeabilized with 0.1% Triton X-100 + 5% BSA (both from Sigma-Aldrich, St. Louis, MO, USA) for 20 min at RT and incubated in dark with 1 unit of Alexa488 Phalloidin (Thermo Fisher Scientific, Waltham, USA) for 1 h at RT. After washing, the cells were mounted in Vectashield (Vector Laboratories, Burlingame, CA, USA) medium to prevent bleaching.

Nanotube formation and actin pattern were visualized with superresolution Zeiss Elyra S1 Structured Illumination Microscope (SIM) ($d_{\text{lat}} \sim 80\text{--}90\text{ nm}$) at 63x magnification (oil immersion objective; N.A.: 1.4) with the Z-stack function to optically slice the cells. Images were acquired with five grid rotations. Records were further analyzed with ImageJ (FIJI; Wayne Rashband, NIH, Washington, USA) and occasionally Imaris 8.2 (Bitplane, Zürich, Switzerland) softwares.

The number of NT-growing cells was counted manually in each field. Occurrence frequencies were calculated from 50 images/sample and given as mean \pm SD. The frequency of nanotube forming cells were calculated as a ratio of cells growing at least one nanotube per all cells visible in the particular field. Cell shape, length and thickness of NTs of



TR100 treated cells were also measured and compared to the values of untreated cells. Length was determined as a distance between the growth cones of the NTs, thickness was measured at three points in each tube: right behind the growth cones and in the middle, the thickness was given as the arithmetic mean of the measured values. Statistical calculations, including significance tests (using Student *t*-test), were made with Excel and Origin 2018 statistical softwares, respectively.

3. RESULTS AND DISCUSSION

In our study changes in cell and NT morphology were measured both in TR100-treated and untreated (control) B cell population. The effect of DMSO was previously tested on control cells, to exclude its toxic effects. Our data suggest that DMSO has no negative effect on the cells even at concentration of 50 μM (data not shown). Therefore – as TR100 was dissolved in DMSO – to provide the same conditions in control and in treated cells, DMSO was added to the medium of the control cells in an amount equal to that of TR100.

Treatment with TR100 resulted in slightly different effects depending on the phase of nanotube formation. B cells adhere to fibronectin coat within 30–45 min due to the interactions between cell surface $\alpha_5\beta_1$ integrins and the components of the fibronectin extracellular matrix. NT growth is initiated after the attachment and saturates within ~ 2 h [14]. In part of our experiments, TR100 was added to the culture after the adhesion of the plated cells to the fibronectin to study the effect of the agent at the early phase of NT development. In the other part of our experiments, TR100 treatment was performed on cells with a well-developed NT network (i.e. TR100 was added to the cells two hours after adhesion to fibronectin). When TR100 was added before the growth of nanotubular bridges it caused more spectacular effects, compared to the changes it produced on cells with complex nanotube networks (Fig. 1). In the early stage of NT formation TR100 in lower (2 μM) concentration remarkably increased (9% vs. 19%) the NT forming capability of B cells (Fig. 2a), while at higher concentration (20 μM) no alteration was observed in their frequency after the 2 h long incubation. Effects of TR100 treatment were also controversial on the morphology of the NTs, while addition of TR100 shortened the tubes in a

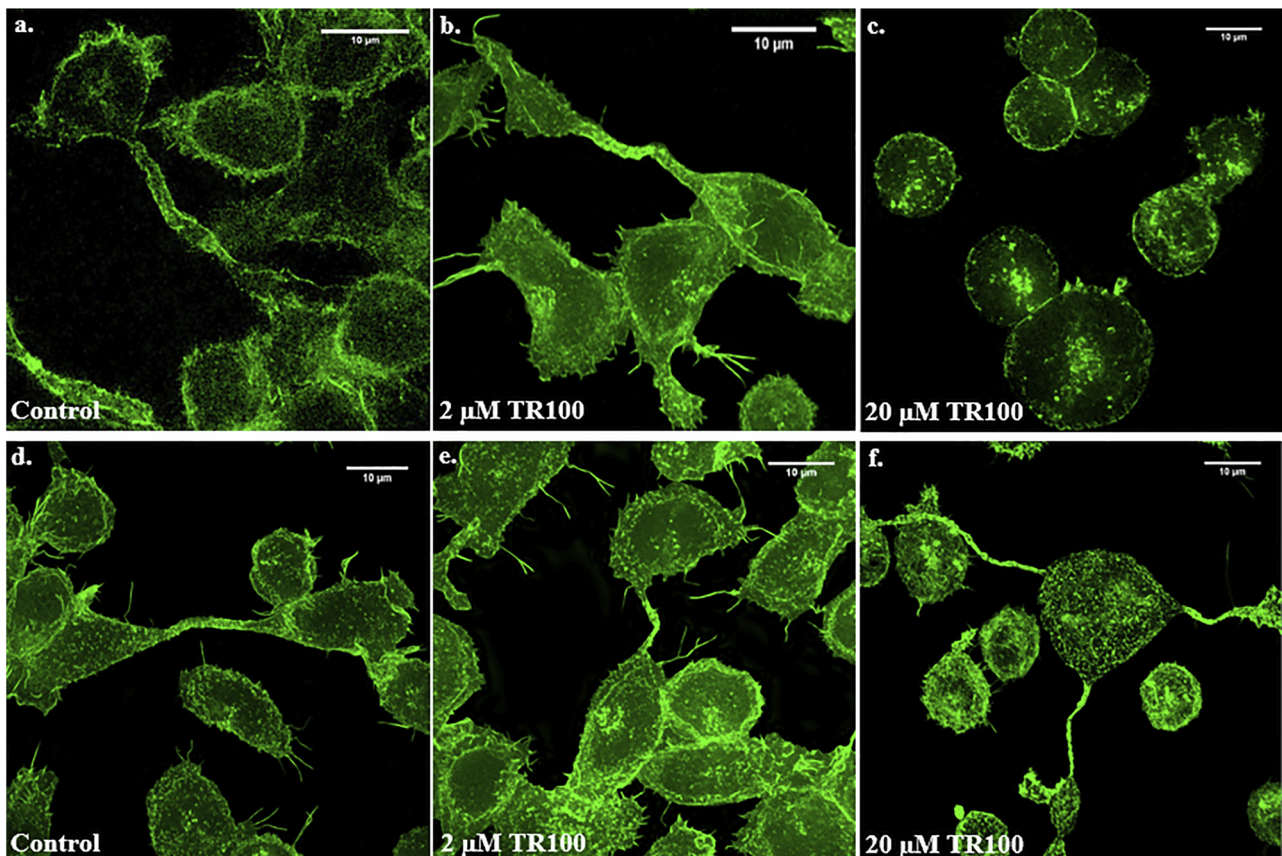
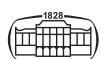


Fig. 1. Effect of treatment on B cells when TR100 was added before the formation of NTs (a–c.) and after extended NT network was formed (d–f). Morphology of cells remained unchanged due to treatment with low dose of TR100 (b., e.), however cells became rounder after the addition of TR100 in higher (20 μM) concentration (c., f). Incubation for longer period of time in the presence of 20 μM TR100 had dramatic effect not only on the cell shape and on the number of membrane projections, but the rearrangement of the actin pattern could also be observed (c.). Cells were fixed then labelled with Alexa fluor488 Phalloidin; visualization was performed with Zeiss Elyra S1 SIM at 63x magnification with 5 grid rotations. Scale bar: 10 μm



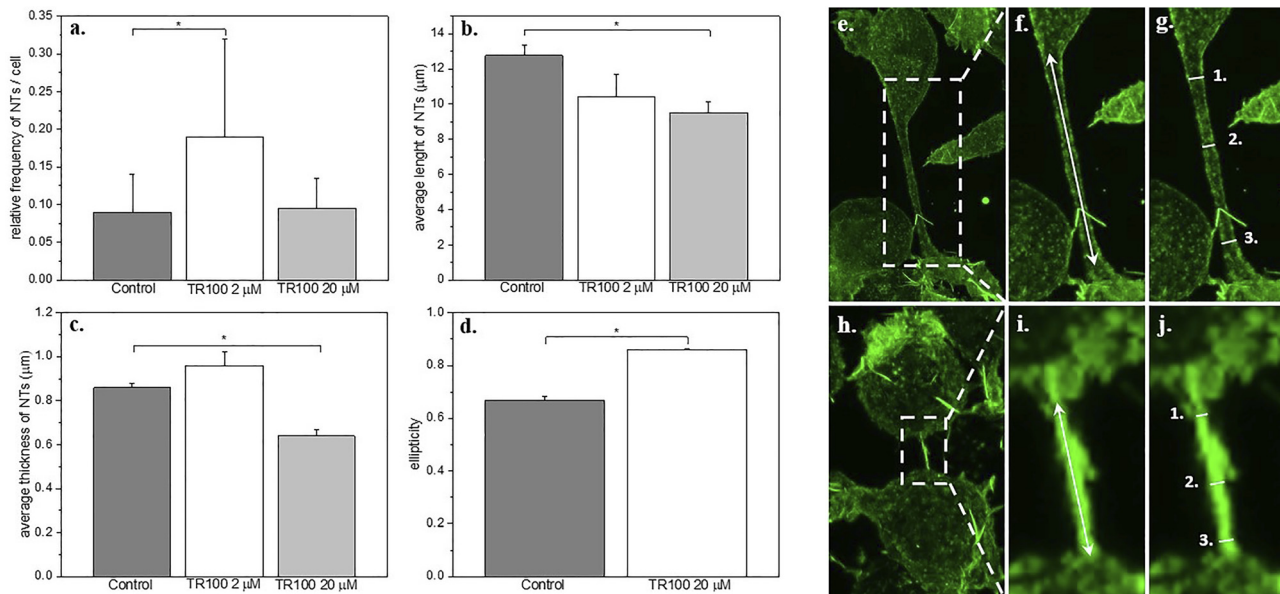


Fig. 2. Effect of TR100 treatment on the morphology of cells and NTs in the early stage of NT formation. TR100 in lower concentration induced NT formation, while higher amount of TR100 did not cause any change in the number of NTs/cell (a). Length of NTs altered in a TR100 concentration dependent manner and resulted in the shortening of the nanotubular bridges (b), while TR100 in 2 μM produced slightly thicker tubes, their width was significantly smaller due to larger concentration of TR100 (c). Longer exposure (6h) to higher concentration (20 μM) of TR100 caused the rounding of the cells (d). Ellipticity (roundness) of cells was calculated with Imaris 8.2 software according to the formula: $f_{\text{circ}} = \frac{4\pi A}{p^2}$, where 'A' is the surface and 'p' is the perimeter of the cells, a value closer to 1 represents more round shape (d). Length and thickness of NTs of TR100 treated cells were analyzed by Fiji and compared to the values of untreated cells (e, h). Length was determined as a distance between the growth cones of the NTs (f, white arrow), or in the absence of these cones as a distance between the end points of the tube (i, white arrow), thickness was measured at three points in each tube: right behind the growth cones and in the middle (g, j, white lines and numbers), the thickness was calculated as the arithmetic average of the measured values (Images f–g. are zoomings of the defined area of image e.; panels i–j. are magnifications of the specified region in image h.) (*: $P < 0.05$)

concentration dependent manner ($12.75 \mu\text{m} \pm 0.63 \mu\text{m}/\text{control}/$ vs. $10.4 \mu\text{m} \pm 1.82 \mu\text{m}/2 \mu\text{M TR100}/$ vs. $9.53 \mu\text{m} \pm 0.59 \mu\text{m}/20 \mu\text{M TR100}/$) (Fig. 2b), their thickness varied in opposite ways: low amount of TR100 thickened, large amount of it thinned the tubes ($0.86 \mu\text{m} \pm 0.02 \mu\text{m}/\text{control}/$ vs. $0.96 \mu\text{m} \pm 0.06 \mu\text{m}/2 \mu\text{M TR100}/$ vs. $0.64 \mu\text{m} \pm 0.03 \mu\text{m}/20 \mu\text{M TR100}/$) (Fig. 2c). In contrast, extended period of incubation (6 h) with 20 μM of TR100 proved to be toxic, resulting in a decrease in the number of the cells, even the majority of the cells became round (0.67 ± 0.013 vs. 0.86 ± 0.004) (Fig. 2d), nanotubes and other membrane projections were present only in a small number (Fig. 1c). TR100

treatment in 20 μM concentration altered the actin pattern as well. Actin seemed to be concentrated into the center of the cells (Fig. 1c). In contrast, neither the length of NTs nor their thickness showed significant deviation from the control samples due to TR100 treatment of cells with extended NT network ($12.15 \mu\text{m} \pm 1.78 \mu\text{m}/\text{control}/$ vs. $11.07 \mu\text{m} \pm 0.75 \mu\text{m}/2 \mu\text{M TR100}/$ vs. $10.28 \mu\text{m} \pm 1.86 \mu\text{m}/20 \mu\text{M TR100}/$, and $0.94 \mu\text{m} \pm 0.04 \mu\text{m}/\text{control}/$ vs. $1.04 \mu\text{m} \pm 0.06 \mu\text{m}/2 \mu\text{M TR100}/$ vs. $0.95 \mu\text{m} \pm 0.08 \mu\text{m}/20 \mu\text{M TR100}/$, respectively) (Fig. 3a and b), however, we have to note that changes in the features of the tubes showed a similar trend to the results obtained when the cells were treated with different

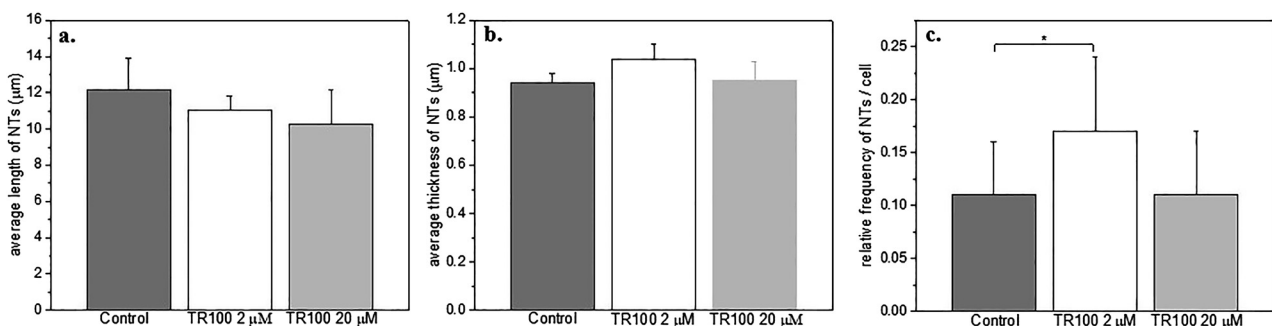


Fig. 3. Effect of TR100 treatment on the morphology of NTs on well-structured NT networks. TR100 did not cause remarkable changes on the shape of NTs (a and b), however low concentration of TR100 triggered NT development (c). (*: $P < 0.05$)



concentrations of TR100 before the growth of the nanotubes. In addition, 2 μM of TR100 significantly increased the NT forming capability of B cells, however this effect was not observed after addition of 20 μM of the drug, and it did not cause any alteration in the NT growth frequency compared to the control ($0.11 \pm 0.05/\text{control}/$ vs. $0.17 \pm 0.07/2 \mu\text{M TR100}/$ vs. $0.11 \pm 0.06/20 \mu\text{M TR100}/$) (Fig. 3c). We have to note that these findings are similar to the results obtained when TR100 was added to the cells before the inception of nanotubes.

TR100 induces the shortening of membrane nanotubes by its effect on the actin cytoskeleton. Its influence prevails primarily in the initial formation of nanotubes. These effects are presumably due to the actin depolymerization action of TR100, causing the disfunction of the normal actin conformation. B cell nanotubes require F-actin for their formation [14, 15], and an impaired cytoskeleton is not able to induce the growth of membrane protrusions, however, change in the actin pattern and decrease in the NT forming capability was observed only after expose the cells to higher concentration of TR100 for a longer period of time. Interestingly, TR100 treatment on cells already developed the nanotubular network was not effective. Bonello et al. in 2016 published that TR100 is incorporated into the growing actin filament during the elongation phase of its polymerization, suggesting that the effects of TR100 cannot be observed on the pre-formed actin filaments. This observation can explain the difference in our data, namely, TR100 was more effective on cells before NT development, while cells after the tube formation was mostly unaffected. TR100 seemed to be highly selective destroying only malignant cells and tissues. NTs were described to help the progression of metastasis and the spreading of resistance factors among cancer cells, therefore NTs could have been a good target of TR100 anti-cancer drug to improve the success of chemotherapy. Despite the above, our data did not support the effectivity of TR100 in the elimination of the tumor cells, and actin based cellular protrusions. In addition, our data suggest that TR100 is ineffective on well-developed nanotube network, indicating that its effect is not sufficient in the case of an advanced process.

4. CONCLUSION

The potential of TR100 in anti-cancer therapy was published a few years ago, because its selectivity and destructive effect on malignant tumors. NTs – communication channels between many cell types, including cancer cells – were demonstrated to be important structures in tumor growth and survival. Although, TR100 was unquestionably a good candidate of a potent therapeutical drug as by affecting the microfilament system and primarily the Tpm3.1 isoform of tropomyosins it can cause the disfunction of tumor cells' cytoskeleton, consequently may inhibit membrane nanotube formation, we were the first who examined the effect of TR100 on NTs and B cells. We showed that it has no remarkable effect on cells with developed NT network, and has only restricted effect on cells in the early phase of NT

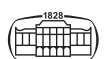
development which raises the possibility that a more powerful drug would be worth looking for. Although, application of TR100 in higher concentration or for extended time may clarify its effect on the formation and function of NTs, its clinical use has been discarded recently. In spite of all these, it cannot be ruled out that TR100 exerts cell-damaging effect by influencing the transport processes mediated by nanotubes. It is important to mention that only B cell NTs were measured in this study, and no other cell lines were investigated. It cannot be ruled out that TR100 shows different impact on NTs of other cells, especially considering that various cell types form nanotubes with different mechanisms. Effect of TR100 on actin-binding proteins also needs to be clarified in the future as these proteins have large influence on the formation of NTs. Furthermore, we have to note that TR100 has contrary effect on B cells' membrane nanotubes comparing with some other anti-cancer drugs, while other agents increased cell survival and the number of intercellular nanotubes [34], and low amount of TR100 can also trigger NT formation, it might result in an obvious decrease in the NT number in higher concentration and do not support cell survival.

ACKNOWLEDGEMENTS

The authors would like to thank to prof. Peter Gunning (UNSW, School of Medical Sciences, Sidney, Australia) and dr. Beáta Bugyi (University of Pécs, Medical School, Department of Biophysics) to have made TR100 available to us. This work was supported by GINOP-2.3.2-15-2016-00036, ÚNKP-21-3-II New National Excellence Program of the Ministry for Innovation and Technology from the Source of the National Research, Development and Innovation Fund (to HH). The research was performed in collaboration with the Nano-Bio-Imaging core facility at the Szentágotthai Research Centre of the University of Pécs.

REFERENCES

1. D. M., Davis; S., Sowinski Membrane nanotubes: dynamic long-distance connections between animal cells. *Nat. Rev. Mol. Cel Biol.* **2008**, *9*, 431–6. <https://doi.org/10.1038/nrm2399>.
2. Rustom, A.; Saffrich, R.; Markovic, I.; Walther, P.; Gerdes, H.-H. Nanotubular highways for intercellular organelle transport. *Science* **2004**, *303*(5660), 1007–10; <https://doi.org/10.1126/science.1093133>.
3. Dupont, M.; Souriant, S.; Lugo-Villarino, G.; Maridonneau-Parini, I.; Vérollet, C. Tunneling nanotubes: Intimate communication between myeloid cells. *Front. Immunol.* **2018**, *9*(JAN), 1–6; <https://doi.org/10.3389/fimmu.2018.00043>.
4. Sowinski, S.; Jolly, C.; Berninghausen, O.; Purbhoo, M. A.; Chauveau, A.; Köhler, K.; Oddos, S.; Eissmann, P.; Brodsky, F.; Hopkins, C.; Onfelt, B.; Sattentau, Q.; Davis, D. M. Membrane nanotubes physically connect T cells over long distances presenting a novel route for HIV-1 transmission. *Nat. Cel Biol.* **2008**, *10*(2), 211–9. <https://doi.org/10.1038/ncb1682>.



5. Chauveau, A.; Aucher, A.; Eissmann, P.; Vivier, E.; Davis, D. M. Membrane nanotubes facilitate long-distance interactions between natural killer cells and target cells. *Proc. Natl. Acad. Sci. United States America* **2010**, *107*(12), 5545–50; <https://doi.org/10.1073/pnas.0910074107>.
6. Wang, Y.; Cui, J.; Sun, X.; Zhang, Y. Tunneling-nanotube development in astrocytes depends on p53 activation. *Cel Death Differ.* **2011**, *18*(4), 732–42; <https://doi.org/10.1038/cdd.2010.147>.
7. Ranzinger, J.; Rustom, A.; Heide, D.; Morath, C.; Schemmer, P.; Nawroth, P. P.; Zeier, M.; Schwenger, V. The receptor for advanced glycation end-products (RAGE) plays a key role in the formation of nanotubes (NTs) between peritoneal mesothelial cells and in murine kidneys. *Cel Tissue Res.* **2014**, *357*(3), 667–79; <https://doi.org/10.1007/s00441-014-1904-y>.
8. Marzo, L.; Gousset, K.; Zurzolo, C. Multifaceted roles of tunneling nanotubes in intercellular communication. *Front. Physiol.* **2012**, *3*; <https://doi.org/10.3389/fphys.2012.00072>.
9. Schiller, C.; Diakopoulos, K. N.; Rohwedder, I.; Kremmer, E.; von Toerne, C.; Ueffing, M.; Weidle, U. H.; Ohno, H.; Weiss, E. H. LST1 promotes the assembly of a molecular machinery responsible for tunneling nanotube formation. *J. Cel Sci.* **2012**, *126*(Pt 3), 767–77; <https://doi.org/10.1242/jcs.114033>.
10. Berg, J. S.; Cheney, R. E. Myosin-X is an unconventional myosin that undergoes intrafilopodial motility. *Nat. Cel Biol.* **2002**, *4*(3), 246–50; <https://doi.org/10.1038/ncb762>.
11. Gousset, K.; Marzo, L.; Commere, P.-H.; Zurzolo, C. Myo10 is a key regulator of TNT formation in neuronal cells. *J. Cel Sci.* **2013**, *126*(19), 4424–35; <https://doi.org/10.1242/jcs.129239>.
12. Delage, E.; Cervantes, D. C.; Pénard, E.; Schmitt, C.; Syan, S.; Disanza, A.; Scita, G.; Zurzolo, C. Differential identity of Filopodia and Tunneling Nanotubes revealed by the opposite functions of actin regulatory complexes. *Sci. Rep.* **2016**, *6*(1), 39632. <https://doi.org/10.1038/srep39632>.
13. Jash, E.; Prasad, P.; Kumar, N.; Sharma, T.; Goldman, A.; Sehrawat, S. Perspective on nanochannels as cellular mediators in different disease conditions. *Cell Commun. Signaling* **2018**, *16*(1), 76; <https://doi.org/10.1186/s12964-018-0281-7>.
14. Osteikoetxea-Molnár, A.; Szabó-Meleg, E.; Tóth, E. A.; Oszvald, Á.; Izsépi, E.; Kremlitzka, M.; Biri, B.; Nyitray, M.; Bozót, T.; Németh, P.; Kellermayer, M.; Nyitrai, M.; Matko, J. The growth determinants and transport properties of tunneling nanotube networks between B lymphocytes. *Cell Mol. Life Sci.* **2016**, *73*(23), 4531–45; <https://doi.org/10.1007/s00018-016-2233-y>.
15. Halász, H.; Ghadaksaz, A. R.; Madarász, T.; Huber, K.; Harami, G.; Tóth, E. A.; Osteikoetxea-Molnár, A.; Kovács, M.; Balogi, Z.; Nyitrai, M.; Matkó, J.; Szabó-Meleg, E. Live cell superresolution-structured illumination microscopy imaging analysis of the intercellular transport of microvesicles and costimulatory proteins via nanotubes between immune cells. *Methods Appl. Fluor.* **2018**, *6*(4), 045005; <https://doi.org/10.1088/2050-6120/aad57d>.
16. Ware, M. J.; Tinger, S.; Colbert, K. L.; Corr, S. J.; Rees, P.; Koshkina, N.; Curley, S.; Summers, H. D.; Godin, B. Radiofrequency treatment alters cancer cell phenotype. *Scientific Rep.* **2015**, *5*(1), 1–14; <https://doi.org/10.1038/srep12083>.
17. Nawaz, M.; Fatima, F. Extracellular vesicles, tunneling nanotubes, and cellular interplay: synergies and missing links. *Front. Mol. Biosciences* **2017**, *4*(July), 1–12; <https://doi.org/10.3389/fmolb.2017.00050>.
18. Hendricks, M.; Weintraub, H. Multiple tropomyosin polypeptides in chicken embryo fibroblasts: differential repression of transcription by Rous sarcoma virus transformation. *Mol. Cell Biol.* **1984**, *4*(9), 1823–33; <https://doi.org/10.1128/MCB.4.9.1823>.
19. Hendricks, M.; Weintraub, H. Tropomyosin is decreased in transformed cells. *Proc. Natl. Acad. Sci.* **1981**, *78*(9), 5633–7; <https://doi.org/10.1073/pnas.78.9.5633>.
20. Lin, J. J.; Helfman, D. M.; Hughes, S. H.; Chou, C. S. Tropomyosin isoforms in chicken embryo fibroblasts: purification, characterization, and changes in Rous sarcoma virus-transformed cells. *J. Cel Biol.* **1985**, *100*(3), 692–703; <https://doi.org/10.1083/jcb.100.3.692>.
21. Gunning, P.; O’neill, G.; Hardeman, E. Tropomyosin-based regulation of the actin cytoskeleton in time and space. *Physiol. Rev.* **2008**, *88*(1), 1–35; <https://doi.org/10.1152/physrev.00001.2007>.
22. Lin, J. L.-C.; Geng, X.; Bhattacharya, S. D.; Yu, J.-R.; Reiter, R. S.; Sastri, B.; Glazier, K. D.; Mirza, Z. K.; Wang, K. K.; Amenta, P. S.; Das, K. M.; Lin, J. J.-C. Isolation and sequencing of a novel tropomyosin isoform preferentially associated with colon cancer. *Gastroenterology* **2002**, *123*(1), 152–62; <https://doi.org/10.1053/gast.2002.34154>.
23. Pawlak, G.; McGarvey, T. W.; Nguyen, T. B.; Tomaszewski, J. E.; Puthiyaveetil, R.; Malkowicz, S. B.; Helfman, D. M. Alterations in tropomyosin isoform expression in human transitional cell carcinoma of the urinary bladder. *Int. J. Cancer* **2004**, *110*(3), 368–73; <https://doi.org/10.1002/ijc.20151>.
24. Miyado, K.; Kimura, M.; Taniguchi, S. Decreased expression of a single tropomyosin isoform, TM5/TM30nm, results in reduction in motility of highly metastatic B16-F10 mouse melanoma cells. *Biochem. Biophys. Res. Commun.* **1996**, *225*(2), 427–35; <https://doi.org/10.1006/bbrc.1996.1190>.
25. Takenaga, K.; Nakamura, Y.; Sakiyama, S. Differential expression of a tropomyosin isoform in low- and high-metastatic Lewis lung carcinoma cells. *Mol. Cell Biol.* **1988**, *8*(9), 3934–7; <https://doi.org/10.1128/MCB.8.9.3934>.
26. Takenaga, K.; Nakamura, Y.; Tokunaga, K.; Kageyama, H.; Sakiyama, S. Isolation and characterization of a cDNA that encodes mouse fibroblast tropomyosin isoform 2. *Mol. Cell Biol.* **1988**, *8*(12), 5561–5; <https://doi.org/10.1128/MCB.8.12.5561>.
27. Jalilian, I.; Heu, C.; Cheng, H.; Freittag, H.; Desouza, M.; Stehn, J. R.; Bryce, N. S.; Whan, R. M.; Hardeman, E. C.; Fath, T.; Schevzov, G.; Gunning, P. W. Cell elasticity is regulated by the tropomyosin isoform composition of the actin cytoskeleton. *PLoS One* **2015**, *10*(5), 1–23; <https://doi.org/10.1371/journal.pone.0126214>.
28. Gunning, P. W.; Schevzov, G.; Kee, A. J.; Hardeman, E. C. Tropomyosin isoforms: divining rods for actin cytoskeleton function. *Trends Cel Biol.* **2018**, *15*(6), 333–41; <https://doi.org/10.1016/j.tcb.2005.04.007>.
29. Geeves, M. A.; Hitchcock-DeGregori, S. E.; Gunning, P. W. A systematic nomenclature for mammalian tropomyosin isoforms. *J. Muscle Res. Cel Motil.* **2015**, *36*(2), 147–53; <https://doi.org/10.1007/s10974-014-9389-6>.
30. Bonello, T. T.; Janco, M.; Hook, J.; Byun, A.; Appaduray, M.; Dedova, I.; Hitchcock-DeGregori, S.; Hardeman, E. C.; Stehn, J. R.; Böcking, T.; Gunning, P. W. A small molecule inhibitor of tropomyosin dissociates actin binding from tropomyosin-directed regulation of actin dynamics. *Sci. Rep.* **2016**, *6*. <https://doi.org/10.1038/srep19816>.



31. Stehn, J. R.; Haass, N. K.; Bonello, T.; Desouza, M.; Kottyan, G.; Treutlein, H.; Zeng, J.; Nascimento, P. R.; Sequeira, V. B.; Butler, T. L.; Allanson, M.; Fath, T.; Hill, T. A.; McCluskey, A.; Schevzov, G.; Palmer, S. J.; Hardeman, E. C.; Winlaw, D.; Reeve, V. E.; Dixon, I.; Weninger, W.; Cripe, T. P.; Gunning, P. W. A novel class of anticancer compounds targets the actin cytoskeleton in tumor cells. *Cancer Res.* **2013**, *73*(16), 5169–82; <https://doi.org/10.1158/0008-5472.CAN-12-4501>.
32. Currier, M. A.; Stehn, J. R.; Swain, A.; Chen, D.; Hook, J.; Eiffe, E.; Heaton, A.; Brown, D.; Nartker, B. A.; Eaves, D. W.; Kloss, N.; Treutlein, H.; Zeng, J.; Alieva, I. B.; Dugina, V. B.; Hardeman, E. C.; Gunning, P. W.; Cripe, T. P. Identification of cancer-targeted tropomyosin inhibitors and their synergy with microtubule drugs. *Mol. Cancer Ther.* **2017**, *100*(12), p. molcanther.0873.2016; <https://doi.org/10.1158/1535-7163.MCT-16-0873>.
33. Haimovich, G.; Ecker, C. M.; Dunagin, M. C.; Eggan, E.; Raj, A.; Gerst, J. E.; Singer, R. H. Intercellular mRNA trafficking via membrane nanotube-like extensions in mammalian cells. *Proc. Natl. Acad. Sci.* **2017**, *114*(46), E9873–82; <https://doi.org/10.1073/PNAS.1706365114>.
34. Desir, S.; O'Hare, P.; Vogel, R. I.; Sperduto, W.; Sarkari, A.; Dickson, E. L.; Wong, P.; Nelson, A. C.; Fong, Y.; Steer, C. J.; Subramanian, S.; Lou, E. Chemotherapy-induced tunneling nanotubes mediate intercellular drug efflux in pancreatic cancer. *Sci. Rep.* **2018**, *8*(1), 9484; <https://doi.org/10.1038/s41598-018-27649-x>.

